



Non-repeatability of large plasticity for Fe-based bulk metallic glasses



Weiming Yang^a, Baoan Sun^b, Yucheng Zhao^{a, **}, Qiang Li^c, Long Hou^a, Ning Luo^a, Chaochao Dun^d, Chengliang Zhao^e, Zhanguo Ma^a, Haishun Liu^{a, *}, Baolong Shen^f

^a State Key Laboratory for Geomechanics and Deep Underground Engineering, School of Mechanics and Civil Engineering, School of Sciences, China University of Mining and Technology, Xuzhou 221116, People's Republic of China

^b Department of Mechanical and Biomedical Engineering, City University of Hong Kong, Hong Kong

^c School of Physics Science and Technology, Xinjiang University, Urumqi, Xinjiang 830046, People's Republic of China

^d Department of Physics, Wake Forest University, Winston Salem, NC 27109, USA

^e Key Laboratory of Magnetic Materials and Devices, Ningbo Institute of Materials Technology & Engineering, Chinese Academy of Sciences, Ningbo 315201, People's Republic of China

^f School of Materials Science and Engineering, Southeast University, Nanjing 211189, People's Republic of China

ARTICLE INFO

Article history:

Received 23 October 2015

Received in revised form

21 March 2016

Accepted 22 March 2016

Available online 24 March 2016

Keywords:

Fe-based metallic glasses

Plastic deformation

Shear bands

Self-organized critical state

ABSTRACT

Serrated flow is an essential characteristic of the plastic deformation of metallic glasses. Under restricted loading conditions, the formation and expansion of shear bands act as the serrated flow of stress-strain curves in metallic glasses. In this work, serrated flows in Fe₅₀Ni₃₀P₁₃C₇ glassy samples with different plasticity were studied. The distribution histogram shows a monotonically decreasing trend during the initial deformation stage (i.e., the plastic deformation in the range of 0–8%), whereas in the following deformation stage (i.e., a plastic deformation of 8–14%), the stress drop frequency distribution presents both a monotonically decreasing distribution and a peak shape similar to chaotic dynamics. It is shown that the spatial evolution behavior of shear bands in Fe₅₀Ni₃₀P₁₃C₇ metallic glasses evolved from self-organized critical to chaotic dynamics in the form of serrated flow, which reveals the origin of discrete plasticity of Fe-based bulk metallic glasses. This study has potential applications for understanding the plastic deformation mechanism.

© 2016 Elsevier B.V. All rights reserved.

1. Introduction

As a new type of metallic material, Fe-based bulk metallic glasses (BMGs) fabricated by rapid solidification of a metal alloy process [1,2] normally exhibit high strength [3,4], excellent corrosion resistance [5], and great magnetic properties [6–8]. Therefore, it is believed that Fe-based BMGs will play an important role in aerospace, national defense military, electrical and electronic products, and other areas relating to functional and structural materials [9]. Unfortunately, Fe-based BMGs usually fracture catastrophically even during the elastic deformation stage at room temperature [10], which hinders their widespread applications. Thus, it would be very important to understand the plastic deformation mechanism and the plasticity enhancements for Fe-based BMGs [11–14]. Normally, plastic deformation of crystal materials

under loading is mainly reduced by so-called dislocations [15,16]. On the contrary, there are no grains or grain boundaries in MGs; thus, plastic deformation under loading conditions cannot be well explained using dislocation theory [17]. It is known that the deformation of MGs under loading at room temperature is mainly induced by the formation and expansion of shear bands [18]. As a result, the instability of a shear band could form a crack extension leading to the catastrophic fracture of BMGs. Progress researching the shear band has been made in the past few decades [19–21]. However, it is still unclear what the formation mechanism and spatial evolution behavior of shear bands are, which has limited the non-repeatable plastic deformation especially for Fe-based BMGs. The evolutionary characteristics of a shear band and/or serrated flow still remains unidentified. Recently, Fe–Ni–P–C BMGs with large compressive plasticity at room temperature were synthesized by combining a fluxing treatment and the J-quenching technique [22]. This exploration may pave the way to a systematic understanding of the evolutionary characteristics of shear bands and/or serrated flows in Fe-based BMGs.

In this work, the spatial evolutionary behavior of shear bands in

* Corresponding author.

** Corresponding author.

E-mail addresses: zhaoyc1972@163.com (Y. Zhao), liuhaishun@126.com (H. Liu).

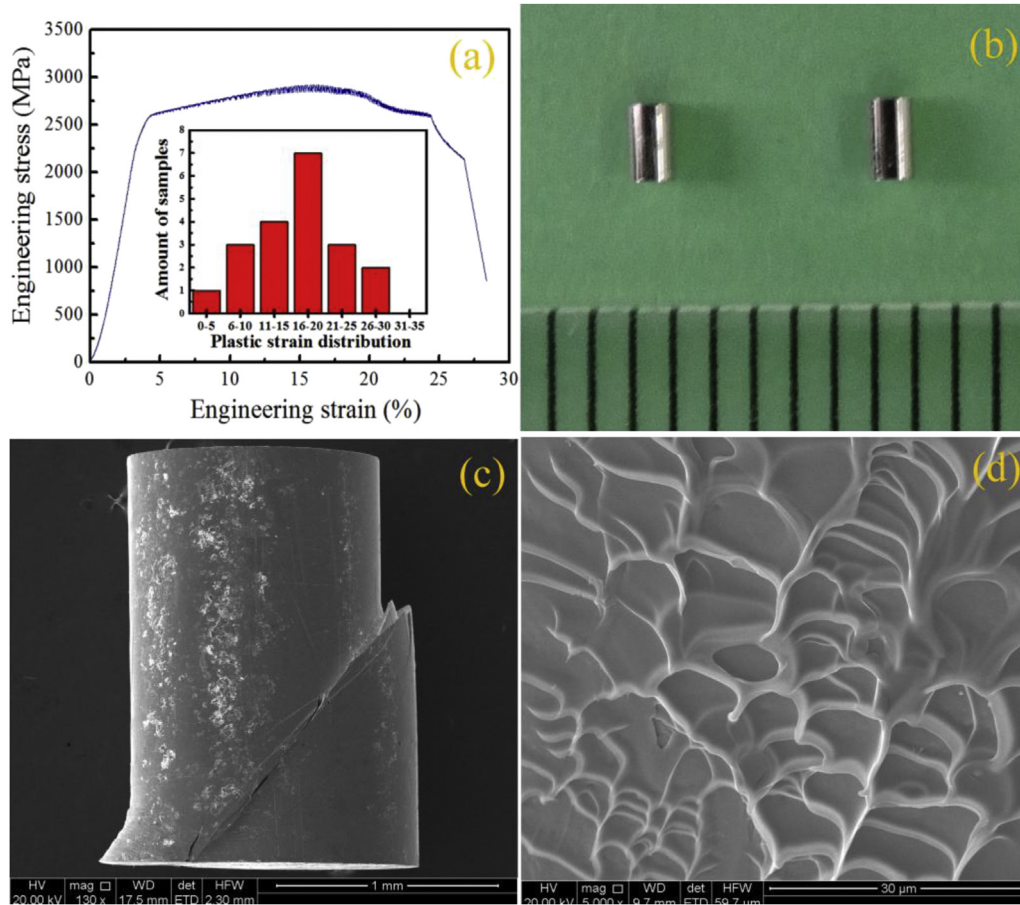


Fig. 1. (a) Stress-strain curves of $\text{Fe}_{50}\text{Ni}_{30}\text{P}_{13}\text{C}_7$ glassy samples at strain rate $5 \times 10^{-4} \text{ s}^{-1}$. (b) The specimen shape and geometric dimension. (c) The SEM image of the $\text{Fe}_{50}\text{Ni}_{30}\text{P}_{13}\text{C}_7$ surface prior to failure. (d) The vein patterns on the shear fracture surface.

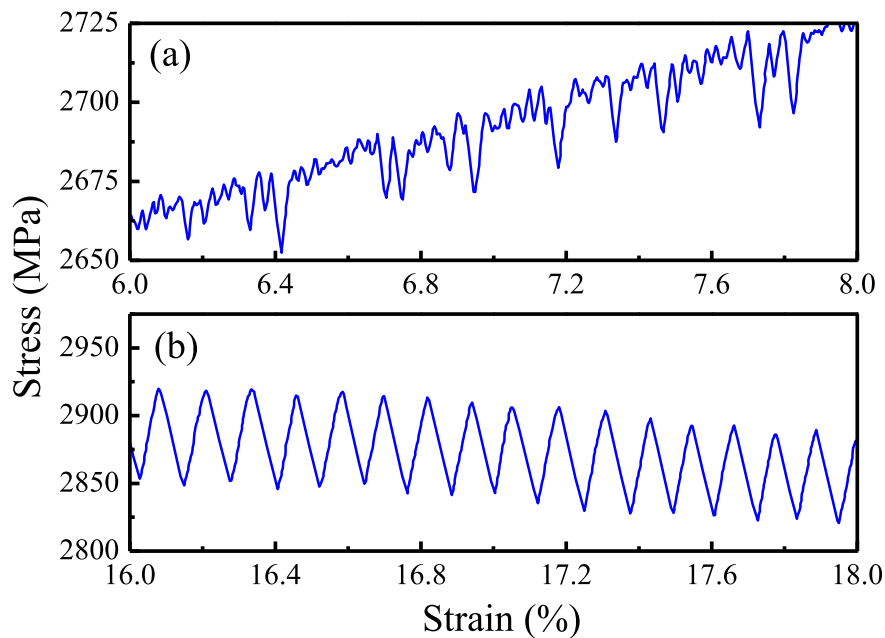


Fig. 2. Comparison of the serrated flows of $\text{Fe}_{50}\text{Ni}_{30}\text{P}_{13}\text{C}_7$ metallic glasses at different strain ranges (a) 6–8% and (b) 16–18%.

$\text{Fe}_{50}\text{Ni}_{30}\text{P}_{13}\text{C}_7$ glassy samples with different plasticity was studied from the viewpoint of dynamic methods. The relationship between

the evolutionary characteristics of serrated flows and their plastic deformation was also established. This work has implications for

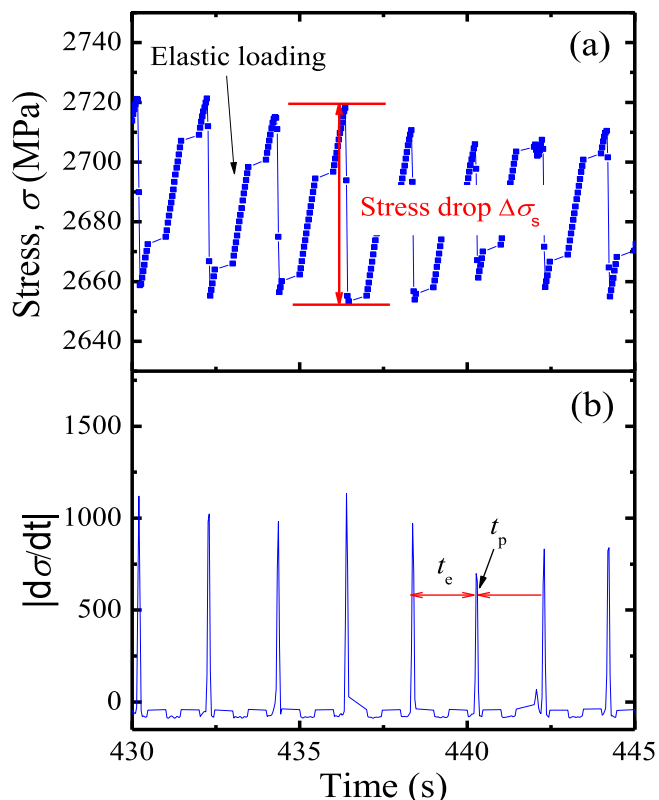


Fig. 3. (a) Stress-time curves for $\text{Fe}_{50}\text{Ni}_{30}\text{P}_{13}\text{C}_7$ metallic glass. (b) Absolute derivative of the stress versus time from (a), which shows the elastic reloading time t_e and the stress drop duration time t_p .

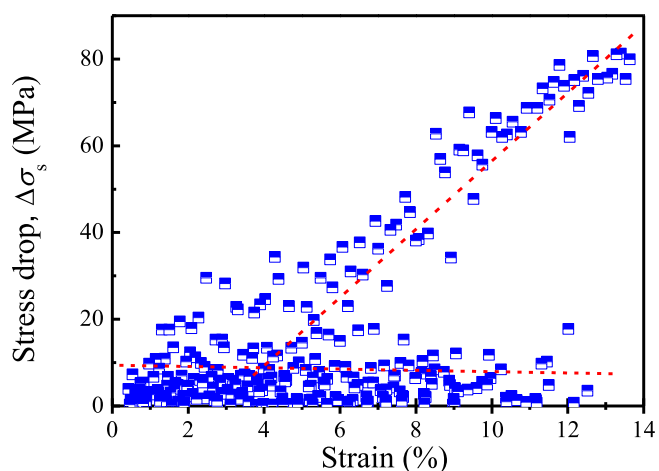


Fig. 4. Distribution of the stress-drops amplitude as a function of the strain for $\text{Fe}_{50}\text{Ni}_{30}\text{P}_{13}\text{C}_7$ metallic glass. Red straight lines crossing the diamonds represent the respective linear fits in two regions. (For interpretation of the references to colour in this figure legend, the reader is referred to the web version of this article).

understanding the precise plastic deformation mechanism of Fe-based BMGs.

2. Experimental

$\text{Fe}_{50}\text{Ni}_{30}\text{P}_{13}\text{C}_7$ BMGs with a diameter of 1.0 mm were prepared by combining fluxing treatment and the J-quenching technique [23]. The nature of glassy samples was ascertained by D8 Advance

X-ray diffraction (XRD) with Cu $K\alpha$ radiation, NETZSCH DSC-404 differential scanning calorimetry (DSC) with a heating rate of 0.67 K/s, high-resolution transmission electron microscopy (HRTEM) and energy dispersive X-ray spectroscopy (EDS) using a Tecnai F20 microscope. The specimens for the compression test were cut from the cast rods, and each end was polished parallel to each other. The mechanical behavior of more than 20 cast samples with a diameter of 1.0 mm and an aspect ratio of 2:1 was examined under uniaxial compression using an Instron testing machine at room temperature with a strain rate of $5 \times 10^{-4} \text{ s}^{-1}$. The tests were carried out in a constant-crosshead-displacement-rate controlled manner. The lateral and fracture surface morphology results were examined by scanning electron microscopy (SEM). In this work, stress vibrations, which were generated by subtracting the linear fitting part from the elastic deformation range, were not included for values greater than 0.5 MPa. Additionally, the serrations with $\Delta\sigma_s < 0.5$ MPa were not counted in our statistics.

3. Results and discussion

Fig. 1(a) shows a representative stress-strain curve of $\text{Fe}_{50}\text{Ni}_{30}\text{P}_{13}\text{C}_7$ glassy samples, and the insets are the statistical distributions of the plastic strains for 20 samples. It can be seen that the $\text{Fe}_{50}\text{Ni}_{30}\text{P}_{13}\text{C}_7$ BMG exhibits extraordinary plasticity, as high as 22%, and different samples possess different plastic strain values. For example, the compressive plastic strain is below 5% for one sample, while they exceed 25% for the other two samples. The specimen shapes and geometric dimensions are given in Fig. 1(b). Fig. 1(c) and (d) show the SEM images of the $\text{Fe}_{50}\text{Ni}_{30}\text{P}_{13}\text{C}_7$ surfaces prior to failure and after compression tests, respectively. Localized main shear bands appear in a near-elliptical morphology and end up at the sample sides, which are characterized by a shear angle of approximately 44° to the compressive axis (Fig. 1(c)). It is noted that several remarkable cracks and scattered shear bands also emerge around the existing primary shear band. These shear bands are not straight but incline to interconnect or intersect with each other. After the compression tests, the exposed sheared surfaces were found to be composed of numerous vein-like patterns, which are a fingerprint of plastic flow (Fig. 1(d)).

It is worth mentioning that the stress-strain curve of $\text{Fe}_{50}\text{Ni}_{30}\text{P}_{13}\text{C}_7$ BMGs has numerous small, serrated distributions, which are not the same as the traditional crystal materials. The stress-strain curves of BMGs reflect the serrated flow behavior and the shear bands have a close relationship with the macroscopic plastic deformation capacity of BMGs. Therefore, by exploring the serrated flow behavior, the spatial evolution behavior of shear bands in $\text{Fe}_{50}\text{Ni}_{30}\text{P}_{13}\text{C}_7$ BMGs is worthy of detailed investigation because the origin of discrete plasticity might be revealed. As an example, Fig. 2 shows the enlarged serrated flow behavior in Fig. 1(a) at strain range 6–8% and 16–18%, respectively. From Fig. 2(a), we can see that different strain values correspond to different serrated flow behavior. In fact, the serrated flow behavior at 6–8% is more complex than the behavior at 16–18%, which has unequal serrated distribution sizes. Moreover, the stress-strain curve of $\text{Fe}_{50}\text{Ni}_{30}\text{P}_{13}\text{C}_7$ BMGs at 6–8% obviously presents the so-called “work hardening” behavior. As is known, the “work hardening” behavior is attributed to the unique structure correlated with the atomic-scale inhomogeneity, leading to an inherent capability of extensive shear band formation, interactions, and multiplication of shear bands [24]. On the contrary, the serrated flow behavior at 16–18% oscillates periodically, with no sign of “work hardening” and only a little decrease in stress intensity, as shown in Fig. 2(b). In this range, only a single dominant shear band is believed to undertake the plastic deformation [25].

To understand the plastic deformation mechanism, Fig. 3 shows

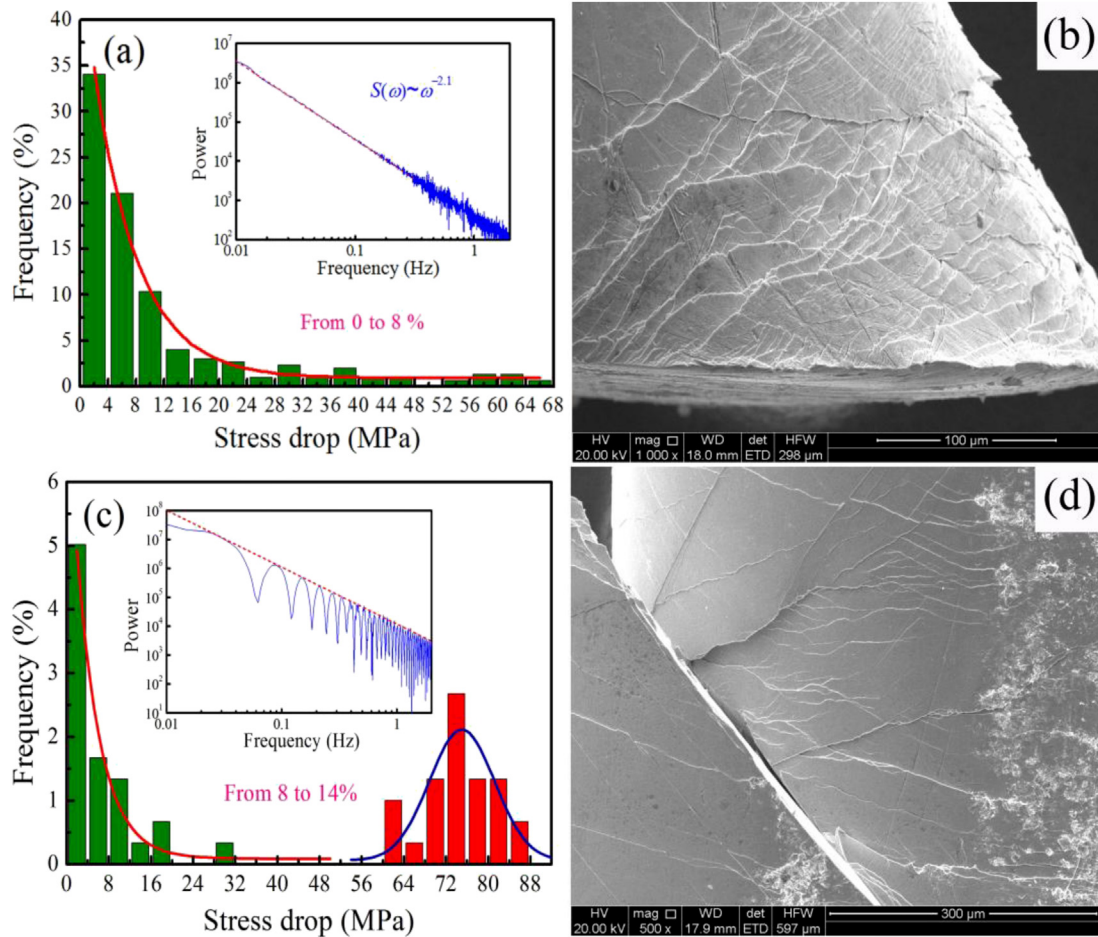


Fig. 5. (a) The statistical distribution of frequency calculated from the continuous strain-stress curves of plastic deformations from 0% to 8%. (b) The shear bands morphology of the self-organized critical state. (c) The statistical distribution of frequency calculated from the continuous strain-stress curves of plastic deformations from 8% to 14%. (d) The shear band morphology of the chaotic state. The insets represent the corresponding power spectrum $S(\omega) \sim \omega$.

a typical stress-time curve for $\text{Fe}_{50}\text{Ni}_{30}\text{P}_{13}\text{C}_7$ BMGs and the corresponding absolute derivative of the stress over time. The serrated stress generally consists of a rising and a declining section, as shown in Fig. 3(a). It is believed that the rising section of the stress represents the elastic reloading process, while the dropping section stands for a real plastic deformation process, i.e., the formation and expansion processes of the shear bands. We can also see that the stress drop duration time t_p is shorter than the elastic reloading time t_e from the derivative of the serrated curve, as shown in Fig. 3(b). Meanwhile, it can be seen that the energy slowly accumulates before the formation and extension of the shear bands. However, once the formation is completed, the shear band will expand rapidly, resulting in the rapid release of energy. At this point in the process, the serrated formation is characterized by the stress drop amplitude $\Delta\sigma_s$. This drop reflects the slippage size of shear bands and depends heavily on the plastic deformation of BMGs. The distribution of $\Delta\sigma_s$ vs. strain for $\text{Fe}_{50}\text{Ni}_{30}\text{P}_{13}\text{C}_7$ BMGs is shown in Fig. 4. It can be seen that $\Delta\sigma_s$ grows slowly with increasing strain, with a small stress serrated behavior appearing in each stage. When the strain reaches a critical value, approximately 8%, the intensive distribution of $\Delta\sigma_s$ disappears and is then gradually divided into two different processes, suggesting the evolvement of the serrated stress from one state to another [26].

These two different processes related to the statistical distribution of frequency and the corresponding shear band morphology

are shown in Fig. 5. In Fig. 5(a), the $\Delta\sigma_s$ presents a monotonic downward trend when the plastic deformation increases from 0% to 8%. The inset of Fig. 5(a) gives the corresponding power spectrum, $S(\omega) \sim \omega^{-\alpha}$, where $\alpha \approx 2.1$, which obeys a power-law distribution with no obvious peak on stress-time. This result reveals that the serrated flow behavior is in the self-organized critical state [19,27]. Fig. 5(b) shows the shear band morphology on the surface of $\text{Fe}_{50}\text{Ni}_{30}\text{P}_{13}\text{C}_7$ BMGs in the self-organized critical state. It can be seen that multiple shear bands are formed in the initial stage of the plastic deformation, with the observed intersection and bifurcation phenomenon that prevent their further propagations. This phenomenon is also the reason that the “work hardening” of $\text{Fe}_{50}\text{Ni}_{30}\text{P}_{13}\text{C}_7$ BMGs exists in this stage. Complex interactions exist among each of the shear bands, leading to a self-organized critical state [17,19]. As is known, the self-organized critical state is a relatively stable dynamic state that has the ability to resist interference. Thus, the system details will have no apparent effect on its stability because the interference caused by additional conditions will be dissipated by interactions among the internal unit. However, the strain, stress, temperature and free volume inevitably change with the increased time in the deformation process. Therefore, the interaction among these parameters will introduce the evolution of the shear bands from a self-organized critical state to chaotic state [27]. In Fig. 5(c), we can see that $\Delta\sigma_s$ presents not only a monotonous downward trend but also the characteristic

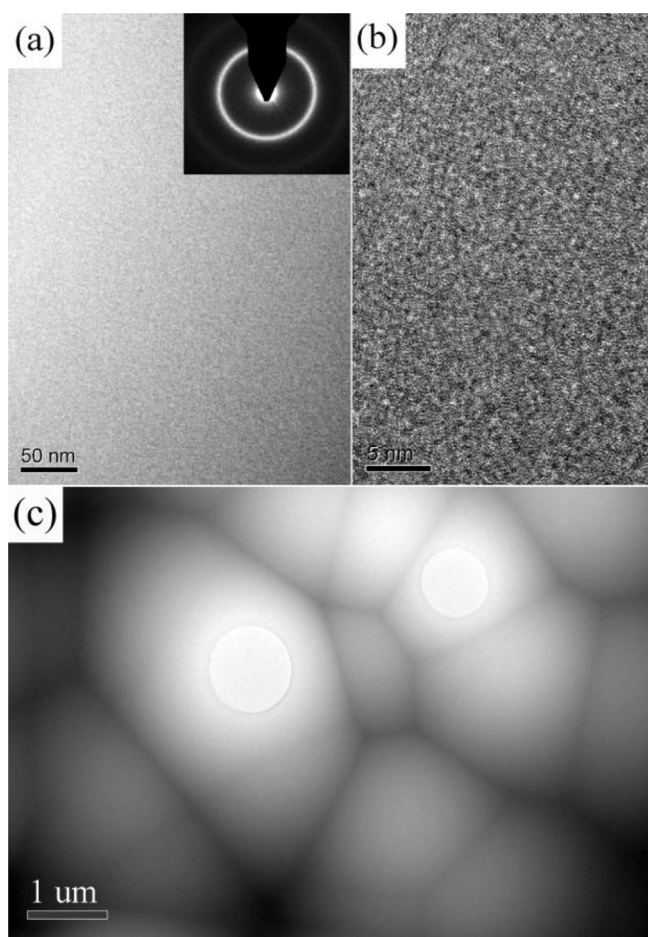


Fig. 6. TEM images of $\text{Fe}_{50}\text{Ni}_{30}\text{P}_{13}\text{C}_7$ sample.

peak shape distribution when the plastic deformation is above 8%. The power spectrum shows obvious peaks with wide noise and the self-similarity structure in the frequency space, indicating the involvement of self-organized critical and chaotic dynamic characteristics in this case [19,27]. As demonstrated in Fig. 5(d), the sample at the chaotic state formed an obvious shear band along the direction that possessed the largest shear stress. Then, the single dominant shear band underwent plastic deformation. Originally, the soft liquid-like layer proceeded in a viscous manner by sliding along the shear plane with elastic energy dissipation, which led to the shear band softening. Once sufficient energy had been dissipated the internal structure of the liquid-like layer began to recover. The solid-like matrix was then reconstructed and the shear band was fully arrested [28–30]. The dynamic softening introduced an increase in the velocity of shear band sliding. With the increased

offset values, the velocity of shear bands also increased, including the temperature in the shear band [31]. When the temperature rose with the energy release due to friction, the thickness of the low viscosity region increased. At a certain critical point, the sample broke down. Such a stochastic process depends on the internal structure and defects in the individual sample. The stochastic formation of a major shear band with large critical offset results in an overcritical rise in temperature and ultimately leads to a catastrophic fracture of the sample [32]. Because the chaotic state is normally unstable, the deformation is actually so sensitive to the initial system that even minor variations of the initial condition may cause huge differences with regards to the final state of the system.

It is known that most of the flow units in BMGs are at an equilibrium state that involves thermal motion behavior when no load is applied. When the BMGs enter the primary stage of plastic deformation, flow units grow constantly, which induce the atomic rearrangement by partial movement of flow units and subsequently the formation of the shear bands. With a constant loading, the probability of overcoming the energy barrier of flow units is increased by thermal activation. As a result, the intersection and self-hindrance triggers the self-organized critical state of shear bands. Moreover, the surrounding atoms are perturbed by the movement of each flow unit, and the shear bands will gradually shift from a self-organized critical state to a chaotic state under continuous loading. Due to the heterogeneity in BMGs [33], it is possible that the huge fluctuations of shear bands could be formed through various nonlinear mechanisms. Because shear bands determine the plastic deformation of BMGs, uncertain characteristics of the plastic strain are then observed from a macroscopic viewpoint. The HRTEM images of $\text{Fe}_{50}\text{Ni}_{30}\text{P}_{13}\text{C}_7$ samples were shown in Fig. 6. No crystalline phase was observed. Moreover, the inserted SAED patterns exhibited a single diffraction halo, with no sharp diffraction rings observed. It was thus confirmed that each sample possessed a complete glassy structure. Fig. 6(c) shows the bright field TEM image of $\text{Fe}_{50}\text{Ni}_{30}\text{P}_{13}\text{C}_7$ samples, including the isolated bright area and the continuous dark area. Among them, the size of the bright area is between 2 and 5 μm , and the width of the dark area is approximately 0.25–1 μm . The strong contrast demonstrates that thickness in the bright area is larger than that of the dark area. In the bright area, voids were observed, revealing the fact that the thinning rate in the bright area is higher than the one in the dark area during the ion thinning process. This might be attributed to the strength difference in these two areas. Using EDS of TEM, the element distributions for bright and dark regions were provided in Table 1. From Table 1, different compositions were observed for the bright area and the dark area outside of the slight deviations from the nominal composition. It is confirmed that even BMGs possessing the same components would cause tiny differences on the structure and element distributions due to the existence of a chaos state, resulting in the uncertainty of plastic strain values for the same BMGs under identical test conditions.

Table 1
Energy dispersive X-ray spectra for bright regions and dark regions.

Area	Element	Weight %	Atomic %	Uncert. %	Detector correction	k-Factor
Bright regions	C	1.03	4.44	0.08	0.26	3.940
	P	7.54	12.59	0.12	0.90	1.068
	Fe	55.29	51.15	0.35	0.99	1.403
	Ni	36.12	31.80	0.29	0.99	1.511
Dark regions	C	0.12	0.57	0.03	0.26	3.940
	P	6.54	11.34	0.10	0.90	1.068
	Fe	57.53	55.33	0.32	0.99	1.403
	Ni	35.79	32.74	0.26	0.99	1.511

4. Conclusions

In this paper, the serrated flow behaviors of Fe₅₀Ni₃₀P₁₃C₇ BMGs were investigated using dynamic methods. It was found that distinct serrated shapes of Fe-based BMGs on stress-strain curves exist during different loading stages. At the initial loading stage, the serrated shapes presented more complicated characteristics compared to before fracturing. When the plastic deformation was below 8%, $\Delta\sigma_s$ presented a monotonous downward trend. In the deformation process, shear bands exist in a self-organized critical state with the serrated behavior showing a power-law distribution within a certain range. In addition to the monotonic downward trend, when the plastic deformation was above 8%, $\Delta\sigma_s$ presented a peak shape distribution indicating a chaotic behavior. The system in the chaotic state is sensitive to the initial conditions, which means that minor differences in the initial conditions may cause vastly different results for the final state of the system. The appearance of the dynamic state may be one of the important reasons for the plastic nature of Fe-based BMGs having a random uncertainty.

Acknowledgments

This work was supported by the National Natural Science Foundation of China (No. 51501220, 51261028 and 51323004) and the Natural Science Foundation of Jiangsu Province (BK20150170, BK20141124 and BK20140178).

References

- [1] D.V. Louzguine-Luzgin, A.I. Bazlov, S.V. Ketov, A.L. Greer, A. Inoue, Crystal growth limitation as a critical factor for formation of Fe-based bulk metallic glasses, *Acta Mater.* 82 (2015) 396–402.
- [2] G. Fiore, M. Baricco, L. Martino, M. Coisson, P. Tiberto, F. Vinai, L. Battezzati, Formation, time-temperature-transformation curves and magnetic properties of FeCoNbSiBP metallic glasses, *J. Alloys Compd.* 619 (2015) 437–442.
- [3] J. Li, W. Yang, D. Estévez, G. Chen, W. Zhao, Q. Man, Y. Zhao, Z. Zhang, B. Shen, Thermal stability, magnetic and mechanical properties of Fe-Dy-B-Nb bulk metallic glasses with high glass-forming ability, *Intermetallics* 46 (2014) 85–90.
- [4] T. Xu, S. Pang, T. Zhang, Glass formation, corrosion behavior, and mechanical properties of novel Cr-rich Cr-Fe-Mo-C-B-Y bulk metallic glasses, *J. Alloys Compd.* 625 (2015) 318–322.
- [5] S.J. Pang, T. Zhang, K. Asami, A. Inoue, Synthesis of Fe-Cr-Mo-C-B-P bulk metallic glasses with high corrosion resistance, *Acta Mater.* 50 (2002) 489–497.
- [6] W.M. Yang, H.S. Liu, L. Xue, J.W. Li, C.C. Dun, J.H. Zhang, Y.C. Zhao, B.L. Shen, Magnetic properties of (Fe_{1-x}Ni_x)₇₂B₂₀Si₄Nb₄ (x=0.0–0.5) bulk metallic glasses, *J. Magn. Magn. Mater.* 335 (2013) 172–176.
- [7] J. Li, J.Y. Law, J. Huo, A. He, Q. Man, C. Chang, H. Men, J. Wang, X. Wang, R.-W. Li, Magnetocaloric effect of Fe-RE-B-Nb (RE = Tb, Ho or Tm) bulk metallic glasses with high glass-forming ability, *J. Alloys Compd.* 644 (2015) 346–349.
- [8] J.W. Li, D. Estévez, K.M. Jiang, W.M. Yang, Q.K. Man, C.T. Chang, X.M. Wang, Electronic-structure origin of the glass-forming ability and magnetic properties in Fe-RE-B-Nb bulk metallic glasses, *J. Alloys Compd.* 617 (2014) 332–336.
- [9] C. Suryanarayana, A. Inoue, Iron-based bulk metallic glasses, *Int. Mater. Rev.* 58 (2013) 131–166.
- [10] J. Shen, Q.J. Chen, J.F. Sun, H.B. Fan, G. Wang, Exceptionally high glass-forming ability of an FeCoCrMoCBy alloy, *Appl. Phys. Lett.* 86 (2005) 151907.
- [11] G. Wang, Y.T. Wang, Y.H. Liu, M.X. Pan, D.Q. Zhao, W.H. Wang, Evolution of nanoscale morphology on fracture surface of brittle metallic glass, *Appl. Phys. Lett.* 89 (2006) 121909.
- [12] X.J. Gu, S.J. Poon, G.J. Shiflet, M. Widom, Ductility improvement of amorphous steels: roles of shear modulus and electronic structure, *Acta Mater.* 56 (2008) 88–94.
- [13] J.T. Kim, S.H. Hong, H.J. Park, Y.S. Kim, G.H. Park, J.-Y. Park, N. Lee, Y. Seo, J.M. Park, K.B. Kim, Improving the plasticity and strength of Fe-Nb-B ultrafine eutectic composite, *Mater. Des.* 76 (2015) 190–195.
- [14] S.F. Guo, J.L. Qiu, P. Yu, S.H. Xie, W. Chen, Fe-based bulk metallic glasses: brittle or ductile? *Appl. Phys. Lett.* 105 (2014) 161901.
- [15] G. Liu, C. Zhang, F. Jiang, X. Ding, Y. Sun, J. Sun, E. Ma, Nanostructured high-strength molybdenum alloys with unprecedented tensile ductility, *Nat. Mater.* 12 (2013) 344–350.
- [16] G. Duscher, M.F. Chisholm, U. Alber, M. Rühle, Bismuth-induced embrittlement of copper grain boundaries, *Nat. Mater.* 3 (2004) 621–626.
- [17] B.A. Sun, W.H. Wang, The fracture of bulk metallic glasses, *Prog. Mater. Sci.* 74 (2015) 211–307.
- [18] A.L. Greer, Y.Q. Cheng, E. Ma, Shear bands in metallic glasses, *Mater. Sci. Eng. R.* 74 (2013) 71–132.
- [19] B.A. Sun, H.B. Yu, W. Jiao, H.Y. Bai, D.Q. Zhao, W.H. Wang, Plasticity of ductile metallic glasses: a self-organized critical state, *Phys. Rev. Lett.* 105 (2010) 035501.
- [20] B.A. Sun, S. Pauly, J. Hu, W.H. Wang, U. Kühn, J. Eckert, Origin of intermittent plastic flow and instability of shear band sliding in bulk metallic glasses, *Phys. Rev. Lett.* 110 (2013) 225501.
- [21] M. Jiang, L. Dai, On the origin of shear banding instability in metallic glasses, *J. Mech. Phys. Solids* 57 (2009) 1267–1292.
- [22] W. Yang, H. Liu, Y. Zhao, A. Inoue, K. Jiang, J. Huo, H. Ling, Q. Li, B. Shen, Mechanical properties and structural features of novel Fe-based bulk metallic glasses with unprecedented plasticity, *Sci. Rep.* 4 (2014) 6233.
- [23] Q. Li, J. Li, P. Gong, K. Yao, J. Gao, H. Li, Formation of bulk magnetic ternary Fe₈₀P₁₃C₇ glassy alloy, *Intermetallics* 26 (2012) 62–65.
- [24] J. Das, M.B. Tang, K.B. Kim, R. Theissmann, F. Baier, W.H. Wang, J. Eckert, “Work-hardenable” ductile bulk metallic glass, *Phys. Rev. Lett.* 94 (2005) 205501.
- [25] J. Pan, Q. Chen, L. Liu, Y. Li, Softening and dilatation in a single shear band, *Acta Mater.* 59 (2011) 5146–5158.
- [26] D.V. Louzguine-Luzgin, V.Y. Zadorozhnyy, N. Chen, S.V. Ketov, Evidence of the existence of two deformation stages in bulk metallic glasses, *J. Non Cryst. Solids* 396–397 (2014) 20–24.
- [27] G. Ananthakrishna, S.J. Noronha, C. Fressengeas, L.P. Kubin, Crossover from chaotic to self-organized critical dynamics in jerky flow of single crystals, *Phys. Rev. E* 60 (1999) 5455–5462.
- [28] H.B. Ke, B.A. Sun, C.T. Liu, Y. Yang, Effect of size and base-element on the jerky flow dynamics in metallic glass, *Acta Mater.* 63 (2014) 180–190.
- [29] Z.Y. Liu, Y. Yang, C.T. Liu, Yielding and shear banding of metallic glasses, *Acta Mater.* 61 (2013) 5928–5936.
- [30] Y. Yang, C.T. Liu, Size effect on stability of shear-band propagation in bulk metallic glasses: an overview, *J. Mater. Sci.* 47 (2012) 55–67.
- [31] J.J. Lewandowski, A.L. Greer, Temperature rise at shear bands in metallic glasses, *Nat. Mater.* 5 (2006) 15–18.
- [32] A.I. Bazlov, A.Y. Churyumov, S.V. Ketov, D.V. Louzguine-Luzgin, Glass-formation and deformation behavior of Ni-Pd-P-B alloy, *J. Alloys Compd.* 619 (2015) 509–512.
- [33] Y.H. Liu, D. Wang, K. Nakajima, W. Zhang, A. Hirata, T. Nishi, A. Inoue, M.W. Chen, Characterization of nanoscale mechanical heterogeneity in a metallic glass by dynamic force microscopy, *Phys. Rev. Lett.* 106 (2011) 125504.